

Fig. 7 Boundaries for linear behavior based on the shock-displacement criteria.

Conclusions

Simulations of unsteady transonic flow over the F-5 wing model were performed in order to study the linearity of unsteady loads and shock displacement with dynamic angle-of-attack amplitude and frequency. The aerodynamic response and shock displacement were found to include higher harmonics, which are usually not considered in correction procedures applied to linear aeroelastic methods.

In flutter analysis there are situations in which a second mode is close to a multiple of a first mode. In such case the presence of a second harmonic in the lower-mode aerodynamic response can facilitate the exchange of energy between the modes and be a contributing factor to coalescence. For this reason the present results seem to indicate the need for considering such harmonics in future correction methods.

Linear boundaries were computed for a few reduced frequencies and spanwise stations along the wing, using two criteria, based on moment coefficient and shock displacement. These boundaries were found to be more conservative for the shock-displacement criterion. The linear limits calculated using the moment coefficient criterion were found to depend significantly on the spanwise station. This indicates that simply using two-dimensional linear limits would not be appropriate when dealing with correction methods.

Notwithstanding the dependence of the linear limits on reduced frequency and spanwise station, it is clear that some degree of linear behavior can be assumed for aeroelastic methods that employ corrected coefficients. However, this assumption of linearity should be used with caution and would not apply to problems such as aeroelastic response or limit cycle, unless the amplitude of deformation is kept below previously identified linear limits that take into account reduced frequency and spanwise station.

Acknowledgments

The authors would like to thank Luciano Amaury dos Santos for his help in processing the data. The second and third authors were supported by the Conselho Nacional de Desenvolvimento Científico e Tecnológico (CNPq), Brazil, under the Integrated Project Research Grant No. 522.413/96-0.

References

- Landahl, M. T., *Unsteady Transonic Flow*, Pergamon, New York, 1951.
- Whitlow, W., Jr., "Computational Unsteady Aerodynamics for Aeroelastic Analysis," NASA TM-100523, Dec. 1987.
- Ashley, H., "Role of Shocks in the 'Sub-Transonic' Flutter Phenomenon," *Journal of Aircraft*, Vol. 17, No. 3, 1980, p. 187.
- Sankar, L. N., Bharadvaj, B. K., and Tsung, F.-L., "A Three Dimensional Navier-Stokes/Full-Potential Coupled Analysis for Viscous Transonic Flows," *AIAA Journal*, Vol. 31, No. 10, 1993.
- Liu, D. D., Kao, Y. F., and Fung, K. Y., "An Efficient Method for Computing Unsteady Transonic Aerodynamics of Swept Wings with Control Surfaces," *Journal of Aircraft*, Vol. 25, No. 1, 1988, pp. 25–31.
- Baker, M. L., Yuan, K., and Goggin, P. J., "Calculation of Corrections to Linear Aerodynamic Methods for Static and Dynamic Analysis and Design," AIAA Paper 98-2072, 1998.

⁷Pitt, D. M., and Goodman, C. E., "Flutter Calculations Using Doublet Lattice Aerodynamics Modified by the Full Potential Equations," AIAA Paper-87-0882-CP, 1987.

⁸Silva, R. G. A., Mello, O. A. F., and Azevedo, J. L. F., "Transonic Flutter Calculations Based on Assumed Mode Shapes Corrections," *Proceedings of the CEAS/AIAA International Forum on Aeroelasticity and Structural Dynamics*, AIAA, Reston, VA, 2001, pp. 183–194.

⁹Dowell, E. H. (ed.), Crawley, E. F., Curtiss, H. C., Jr., Peters, D. A., Scanlan, R. H., and Sisto, F., *A Modern Course in Aeroelasticity*, 3rd ed., Kluwer, Dordrecht, The Netherlands, 1995, pp. 472–487.

¹⁰Sankar, L. N., and Kwon, O. J., "High-Alpha Simulation of Fighter Aircraft," *Proceedings of the NASA High Angle-of-Attack Technology Conference*, Vol. 1, Pt. 2, NASA Langley Research Center, Hampton, VA, 1990, pp. 689–702.

¹¹Mello, O. A. F., and Sankar, L. N., "Computation of Unsteady Transonic Flow over a Fighter Wing Using a Zonal Navier-Stokes/Full-Potential Method," *International Journal for Numerical Methods in Fluids*, Vol. 29, No. 5, 1999, pp. 575–585.

¹²Tijdeman, H., van Nunen, J. W. G., Kraan, A. N., Persoon, A. J., Poestkoke, R., Roos, R., Schippers, P., and Siebert, C. M., "Transonic Wind Tunnel Tests on an Oscillating Wing with External Stores, Part II: Clean Wing," Air Force Flight Dynamics Lab., AFFDL-TR-78-194, Part II, Wright-Patterson AFB, OH, 1979; also NLR-TR-78106-U, Part II.

¹³Palacios, R., Climent, H., Karlsson, A., and Winzell, B., "Assessment of Strategies for Correcting Linear Unsteady Aerodynamics Using CFD or Test Results," *Proceedings of the CEAS/AIAA International Forum on Aeroelasticity and Structural Dynamics*, AIAA, Reston, VA, 2001, pp. 195–210.

Advantages of a Bristled Wing as a Rotary Wing

S. Sunada*

Osaka Prefecture University, Osaka 599-8531, Japan

K. Kawachi†

University of Tokyo, Tokyo 113-8656, Japan

and

K. Yasuda‡

Nihon University, Chiba 274-8501, Japan

Introduction

RECENTLY, the Defense Advanced Research Projects Agency in the United States proposed developing a centimeter-sized insect-like flying machine.^{1–3} In the future millimeter-sized flying machines will be indispensable for obtaining information in environments not readily accessible to people, such as hazardous or confined areas. Sunada et al.⁴ recently studied the flight of the thrips, which is a millimeter-sized insect. They investigated the fluid-dynamic characteristics of a model bristled wing whose planform is proportional to that of a real thrips' fore wing and where cylinders are used to simulate actual bristles. The characteristics were then compared with those of a solid wing whose planform included the addition of membranes between the cylinders of the wing. Their results reveal that the fluid-dynamic forces acting on the bristled wing are smaller than those on the solid wing during constant-velocity translation.

Received 5 December 2002; revision received 30 May 2003; accepted for publication 5 June 2003. Copyright © 2002 by the American Institute of Aeronautics and Astronautics, Inc. All rights reserved. Copies of this paper may be made for personal or internal use, on condition that the copier pay the \$10.00 per-copy fee to the Copyright Clearance Center, Inc., 222 Rosewood Drive, Danvers, MA 01923; include the code 0021-8669/03 \$10.00 in correspondence with the CCC.

*Associate Professor, Department of Aerospace Engineering, Graduate School of Engineering; sunada@aero.osakafu-u.ac.jp.

†Professor, Department of Aeronautics and Astronautics, Associate Fellow AIAA.

‡Associate Professor, Department of Aerospace Engineering, College of Science and Technology, Senior Member AIAA.

accelerated translation, constant-velocity rotation, and accelerated rotation, and that the ratio of the fluid-dynamic forces between the bristled wing and the solid wing is between 0.8 and 1, independent of the type of wing motion. However, the fluid-dynamic force coefficients for the bristled wing are larger than those for the solid wing, because of the difference between the wing surface areas.

In this study we show that the higher force coefficients of a bristled wing are advantageous because they induce a smaller inertial force. Here, first we obtain an analytical expression for a ratio of centrifugal forces between any two bristled wings generating the same lift. The model bristled wings have cylinders to simulate actual bristles. Then, we measure the lift coefficients on bristled wings for various distances between neighboring cylinders to determine the ratio of centrifugal forces. Next, by using the analytical and experimental results we clarify how centrifugal force acting on a bristled wing depends the distance between neighboring cylinders. Finally, we show the advantage of a bristled wing by comparing the centrifugal force acting on a bristled wing and that on a solid wing, which is a bristled wing where neighboring cylinders touch each other.

Analytical

Here, an analytical expression is obtained for the ratio of centrifugal forces acting on any two bristled wings (designated wing 1 and wing 2 for clarity) generating the same lift. A solid wing is included in this analysis because a solid wing is considered a bristled wing when the neighboring cylinders touch each other.

Figure 1 shows the configuration for the bristled wings. Both wings 1 and 2 have the same wing length x_w , chord length c , wing thickness t_m , and cylinder diameter d . The value of t_m is equal to that of d . The difference between the wings is the number of cylinders n , and thus the wings differ in the distance between neighboring cylinders D (because x_w is fixed). In this study we use the ratio D/d as a parameter indicating the "bristleness" of a wing; for the solid wing D/d is 1, namely, the cylinders are touching each other.

The two wings are assumed to generate the same lift force during steady rotational motion with a constant angle of attack (constant collective pitch). The angular velocity of rotational motion for wing 1 and wing 2 is ω_1 and ω_2 , respectively. If the two wings are assumed to generate the same lift, then

$$0.5\rho \int_0^{x_w} (x\omega_1)^2 C_1(x) C_{L1} dx = 0.5\rho \int_0^{x_w} (x\omega_2)^2 C_2(x) C_{L2} dx \quad (1)$$

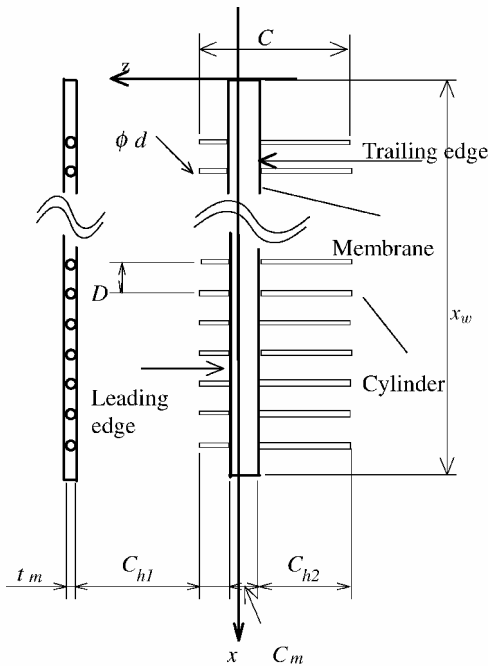


Fig. 1 Model bristled wing where cylinders are used to simulate the bristles.

where C_L is the lift coefficient and ρ is the density of the fluid. $C_1(x)$ and $C_2(x)$ are C where a cylinder is located, and they are C_m where no cylinder is located. Then,

$$C_{L1} S_1 \omega_1^2 \approx C_{L2} S_2 \omega_2^2 \quad (2)$$

where S is the wing surface area. From this equation

$$\omega_1/\omega_2 \approx [(C_{L2}/C_{L1})(S_2/S_1)]^{1/2} \quad (3)$$

The centrifugal force acting on a wing is proportional to wing mass and the second power of ω . Therefore, the ratio of the centrifugal force acting on wing 1 to that on wing 2, K , is

$$K = (m_1/m_2)(\omega_1/\omega_2)^2 = (S_1/S_2)(\omega_1/\omega_2)^2 \quad (4)$$

where m is wing mass. The ratio of the wing mass between these wings is approximately equal to the ratio of their wing surface area because both wings have the same membrane thickness t_m and the same cylinder diameter d . Substituting Eq. (3) into Eq. (4),

$$K = C_{L2}/C_{L1} \quad (5)$$

It is indicated in Ref. 5 that the C_L at $Re \cong 1$ is proportional to $1/Re^k$, and k is a constant close to 1. The Re is proportional to ω in this study because the wing length and the chord length are constant. The C_L is then,

$$C_L \propto 1/Re^k \propto 1/\omega^k \quad (6)$$

The C_{L1} and C_{L2} are lift coefficients at different Reynolds numbers because ω_1 is not equal to ω_2 . Based on Eq. (6), C_{L1} and C_{L2} can be roughly estimated as the lift coefficients of wings 1 and 2 at a common Reynolds number \bar{C}_{L1} and \bar{C}_{L2} , respectively. Then,

$$C_{L2}/C_{L1} = (\bar{C}_{L2}/\bar{C}_{L1})(\omega_1/\omega_2)^k \quad (7)$$

Substituting Eqs. (3) and (7) into Eq. (5), the ratio of the centrifugal force acting on wing 1 to that on wing 2, K , is then

$$K = (\bar{C}_{L2}/\bar{C}_{L1})^{2/(2-k)} (S_2/S_1)^{k/(2-k)} \quad (8)$$

Experimental Details

Materials and Methods

Figure 1 shows the configuration of the model wings. The physical parameters nondimensionalized by chord length c ($= 100$ mm) are as follows:

$$\begin{aligned} x_w/c &= 3, & d/c &= 5 \times 10^{-3}, & c_m/c &= 2 \times 10^{-1} \\ c_{h1}/c &= 1.8 \times 10^{-1}, & c_{h2}/c &= 6.2 \times 10^{-1}, & t_m/c &= 10^{-2} \end{aligned} \quad (9)$$

These nondimensionalized values are similar to those of a real thrips' fore wing.⁶ The model wings differ in n , D/d , and S as follows:

$$[n, D/d, S(\text{mm}^2)] = (6, 101, 6.2 \times 10^3), (26, 20, 7 \times 10^3),$$

$$(51, 10, 8 \times 10^3), (101, 5, 10^4), (251, 2, 1.6 \times 10^4) \quad (10)$$

Among these wings, the wing with $n = 51$ and $D/d = 10$ was the most similar to a real thrips' wing.⁶ The solid wing, which is a bristled wing with $D/d = 1$, is not used in the measurements. A value of K for the solid wing is obtained by extrapolating the values of the bristled wings just stated.

The experimental apparatus and procedure are described in detail in Ref. 4. The wing is moved at a constant forward velocity $V_0 = 6 \times 10^{-2}$ m/s and at a constant angle of attack α in a tank filled with an aqueous solution of glycerin ($\rho = 1.2 \times 10^3$ kg/m³, $\nu = 3 \times 10^{-4}$ m²/s), and the lift and drag acting on the wing are measured. The measurements are made as a function of angle of attack α . For each wing the Reynolds number based on c , $Re(c) = V_0 c / \nu$, is 20, and that based on d , $Re(d) = V_0 d / \nu$, is 0.1. The C_L and C_D

for each wing are calculated by nondimensionalizing the measured lift and drag by the force $0.5\rho V_0^2 S$.

Experimental Uncertainty

The total measurement error is caused by bias errors and precision errors. The bias errors are caused mainly by the load cell and strain amplifier. The maximum bias error is less than 5%. The precision error is mainly caused by errors in measuring the angle of attack and measuring the wing velocity and to the disturbance generated by the wing motion. This error produces scatter in the C_L and C_D data and results in an error of 5%. Therefore, the total measurement error in C_L and C_D is less than $8[\approx (5^2 + 5^2)^{1/2}]%$, which is small enough not to affect our conclusions about the centrifugal forces acting on the wings.

Results and Discussions

Using the analytical expression for K and the C_L obtained from the measurements, centrifugal forces are compared. The K between a bristled wing with $D/d=10$ ($n=51$) and the other wings; the former is used as wing 1, and the latter are used as wing 2, as described in the analytical section.

Figures 2a and 2b show C_L and C_L/C_D as a function of α for various D/d and indicate the following:

- 1) For any D/d , C_L increases with increasing α .
- 2) C_L is maximum when $D/d=10$. (The lift, which is proportional to C_L and the wing surface area S , decreases monotonously as D/d is increased.)
- 3) For any D/d , C_L/C_D is maximum when $\alpha \approx 30$ deg.
- 4) C_L/C_D decreases with increasing D/d .

The thickness of the membrane t_m is two times larger than the diameter of the cylinders d , as shown in Eqs. (9). The effect of this difference in t_m on the measured lift and drag is expected to be small, and thus the measured C_L and C_D are regarded as those of a bristled wing whose membrane thickness is equal to d .

Figure 3 shows K , determined by using \bar{C}_L at $\alpha=20, 45$ deg (Fig. 2) and $k=0.8$. [Results are not strongly affected by

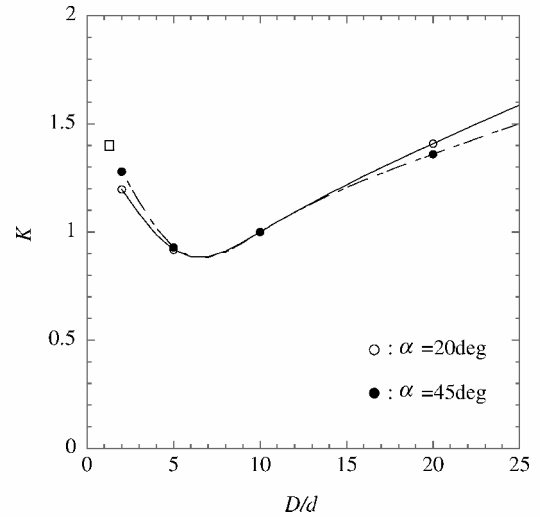


Fig. 3 Ratio of the centrifugal force acting on wing 1 to that on wing 2, K , as a function of the ratio of cylinder distance to cylinder diameter D/d for model bristled wings. K was calculated using $k=0.8$ and using \bar{C}_L values shown in Fig. 2. The rectangle at $D/d=1$ indicates a value by the extrapolation by the other values.

$k(0.5 \leq k \leq 1)$.] K is relatively independent of α . The value of K for a solid wing ($D/d=1$) is estimated to be 1.4 by the extrapolation of the values in this figure. For a bristled wing whose $D/d < 20$, $K < 1.4$. Therefore, the centrifugal force acting on a bristled wing whose $D/d < 20$ is smaller than that acting on a solid wing ($D/d=1$) for the same generated lift. The figure also shows that D/d for minimizing the centrifugal force is about seven.

Conclusions

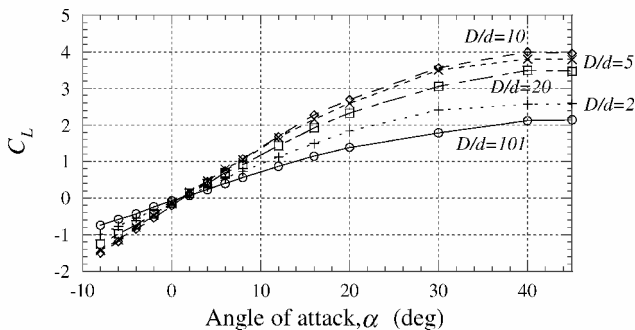
Fluid-dynamic characteristics of model bristled wings are measured under $Re(c) \approx 20$, for various D/d , which is the ratio of the diameter of cylinders d and the distance between neighboring cylinders D . The measurements show that the lift and the lift-to-drag ratio increase with decreasing D/d and that the lift coefficient C_L is maximum at $D/d=10$. This indicates that the centrifugal force acting on a bristled wing whose $D/d < 20$ is less than that acting on a solid wing ($D/d=1$). Thus, a bristled wing shows promise as a rotary wing caused by its smaller centrifugal force when $Re(c) \approx 20$.

Acknowledgment

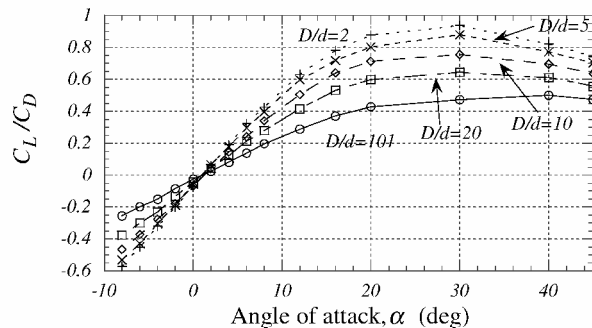
This research was financially supported by Precursory Research for Embryonic Science and Technology, Japan Science and Technology Corporation.

References

- ¹Morris, S. J., and Holden, M., "Design of Micro Air Vehicles and Flight Test Validation," *Proceedings of the Conference on Fixed, Flapping and Rotary Vehicles at Very Low Reynolds Numbers*, edited by T. J. Mueller, Univ. of Notre Dame, Notre Dame, IN, 2000, pp. 153–175.
- ²Kroo, I., and Kunz, P. J., "Meso-Scale Flight and Miniature Rotorcraft Development," *Proceedings of the Conference on Fixed, Flapping and Rotary Vehicles at Very Low Reynolds Numbers*, 2000, pp. 184–196.
- ³Pornsin-Sirirak, T. N., Lee, S. W., Nassef, H., Grasmeyer, J., Tai, Y. C., Ho, C. M., and Keennon, M., "MEMS Wing Technology for a Battery-Powered Ornithopter," *IEEE Micro Electronics Mechanical Systems Technical Digest*, 23–27 Jan. 2000, pp. 799–804.
- ⁴Sunada, S., Takashima, H., Hattori, T., Yasuda, K., and Kawachi, K., "Hydrodynamic Characteristics of Bristled Wings," *Journal of Experimental Biology*, Vol. 205, No. 17, 2002, pp. 2737–2744.
- ⁵White, M. F., *Viscous Fluid Flow*, McGraw-Hill, New York, 1991, pp. 173–184.
- ⁶Tanaka, S., "Aerodynamic Force Acting on Thrips Wings," *Abstracts of Proceedings, Symposia 95, ERATO, JST, Tokyo*, 1995, pp. 27–34.



a)



b)

Fig. 2 Measured lift coefficient C_L and measured lift-to-drag coefficient C_L/C_D , as a function of angle of attack α for various ratios of cylinder distance to cylinder diameter D/d for model bristled wings: a) $\alpha - C_L$ and b) $\alpha - C_L/C_D$.